Improvement in reliability and power consumption based on $Ge_{10}Sb_{90}$ films through erbium doping

Hua Zou, Yifeng Hu, Xiaoqin Zhu, Yuemei Sun, Long Zheng, Yongxing Sui, Shichen Wu & Zhitang Song

Journal of Materials Science
Full Set - Includes `Journal of Materials Science Letters'

ISSN 0022-2461
Volume 52
Number 9

J Mater Sci (2017) 52:5216-5222
DOI 10.1007/s10853-017-0762-x

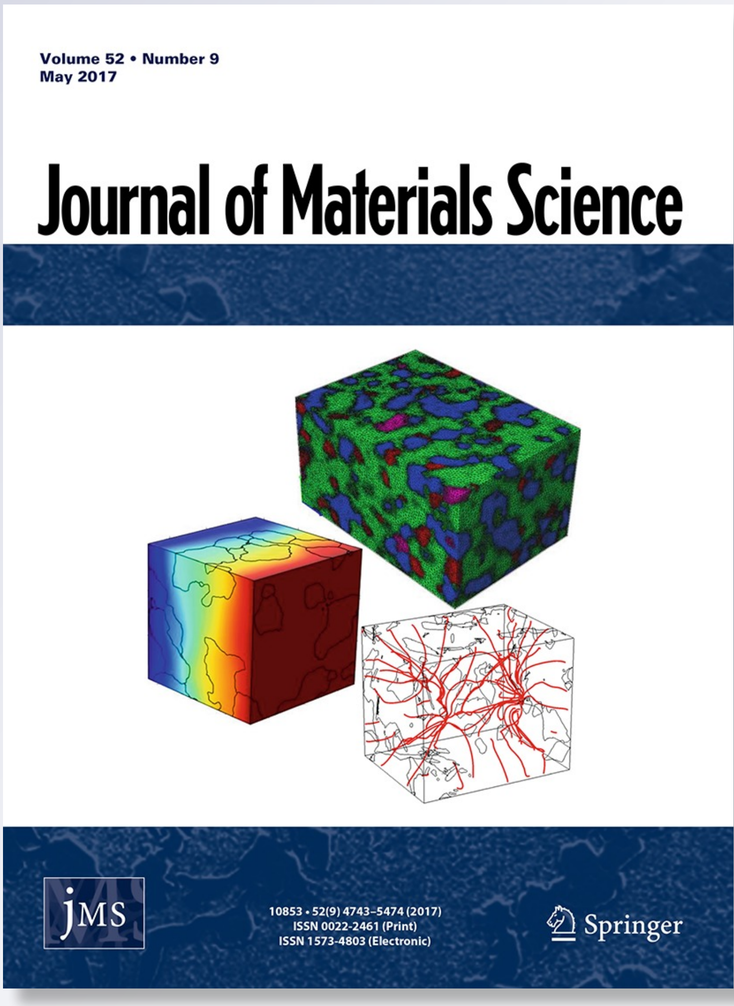

Springer

J Mater Sci (2017) 52:5216–5222

Improvement in reliability and power consumption based on $Ge_{10}Sb_{90}$ films through erbium doping

Hua Zou[1,*], Yifeng Hu[1], Xiaoqin Zhu[1,*], Yuemei Sun[1], Long Zheng[1], Yongxing Sui[1], Shichen Wu[1], and Zhitang Song[2]

[1] School of Mathematics and Physics, Jiangsu University of Technology, Changzhou 213001, People's Republic of China
[2] State Key Laboratory of Functional Materials for Informatics, Shanghai Institute of Micro-system and Information Technology, Chinese Academy of Sciences, Shanghai 200050, People's Republic of China

Received: 18 October 2016
Accepted: 5 January 2017
Published online: 12 January 2017

ABSTRACT

For the application of phase-change materials at nonvolatile memory, it is very desirable to enhance the thermal stability and decrease the power consumption. In our previous work, it has been proved that the Er doping can significantly improve the thermal stability of Sb thin film. In this work, the Er-doped $Ge_{10}Sb_{90}$ thin films were fabricated by magnetron sputtering. It is observed that the crystallization temperatures and 10-year retention temperature of $Ge_{10}Sb_{90}$ films can be significantly improved by Er doping, indicating the improvement in reliability. In addition, the resistances of amorphous and crystalline state of Er-doped $Ge_{10}Sb_{90}$ increase with increasing the Er content, revealing the decrease in writing current of phase-change device based on the film. Last but not least, the phase-change memory cells based on the Er-doped $Ge_{10}Sb_{90}$ film were fabricated and tested, which demonstrated their lower power consumption and excellent switching endurance.

Introduction

As next-generation nonvolatile memory devices, phase-change memory (PCM) has made great progress and attracted much attention over the past decades [1, 2]. The data storage of PCM is achieved by a thermally induced reversible phase transition between amorphous and crystalline state, where the former state represents "0" state (high resistance) and the latter expresses the "1" state (low resistance) [3]. Compared with other memory, the PCM has unique properties such as high speed, low power consumption, perfect data retention capability and fabrication compatibility with complementary metal–oxide–semiconductor (CMOS) technology [3–5].

Recently, PCM development requires the optimization of a serious of parameters including large electrical contrast, high cycle number, good retention and low power [3]. The key factor affecting PCM properties is the characteristic of the phase-change films. Nowadays, the $Ge_2Sb_2Te_5$ (GST) is considered to be the prototype material for PCM application because of their good stability and high speed [6]. However, the Te element is harmful to

Address correspondence to E-mail: zouhua@jsut.edu.cn; pcram@jsut.edu.cn

DOI 10.1007/s10853-017-0762-x

semiconductor techniques due to its volatilization, and the presence of Te will lead to the phase segregation after cycling and insufficient data retention [7]. Thus, the Te-free and Sb-rich GeSb thin films have been considered the promising candidate for replacing GST due to their fast crystallization speed.

Unfortunately, the normal pure GeSb-based PCM cannot maintain good stability and high speed [8, 9]. In order to improve the properties of phase-change films, many experimental attempts have been made [10–13]. Among these works, the doping of phase-change films is very effective to enhance the phase-change properties [5, 14]. So far, dopants of Si [15], N [16], Mg [17], Al [18], Cu [19], etc. have been frequently used to enhance material properties. We pioneered the development that rare earth doping, such as Er, can significantly improve the phase-change properties of Sb thin film [20]. In this work, the rare earth element of erbium (Er) is chosen as dopants for improving the phase-change performance of $Ge_{10}Sb_{90}$ films.

Experimental

The Er-doped $Ge_{10}Sb_{90}$ thin films of $Er_x(Ge_{10}Sb_{90})_{1-x}$ ($0 \leq x \leq 0.024$) were deposited on SiO_2/Si (100) wafers by co-sputtering of Er and $Ge_{10}Sb_{90}$ targets at room temperature using magnetron sputtering. The purity of Sb and $Ge_{10}Sb_{90}$ targets was 99.999%. The base pressure in the deposition chamber was 2×10^{-4} Pa. Sputtering was performed under the Ar gas pressure of 0.3 Pa and the flow of 30 SCCM. The thin film thickness was set to 50 nm through controlling deposition time of $Ge_{10}Sb_{90}$. To ensure the uniformity of deposition, the substrate holder was rotated at an autorotation speed of 20 rpm. The amorphous-to-crystalline transition was investigated by in situ temperature-dependent resistance (R-T) measurement using a TP 95 temperature controller (Linkam Scientific Instruments Ltd., Surrey, UK) under Ar atmosphere. The reflectivity of the films was measured in the range of 400–2500 nm by NIR spectrophotometer (7100CRT, XINMAO, China). The crystalline structures of the films were analyzed by X-ray diffraction (XRD, PANalytical, X'PERT Powder). The surface morphology of the films was examined by atomic force microcopy (AFM, FM-Nanoview 1000). The PCM devices based on the $Er_{0.018}(Ge_{10}Sb_{90})_{0.982}$ thin film with a tungsten heating electrode of 260 nm diameter were fabricated by 0.18-μm CMOS technology. Between the $Er_{0.018}(Ge_{10}Sb_{90})_{0.982}$ film and the top electrode, a 20-nm-thick TiN film was deposited by direct current magnetron sputtering. Current–voltage (I–V), resistance–voltage (R–V) and endurance characteristics were conducted using a Keithley 2400 semiconductor parameter analyzer and an Agilent 81104A programmable pulse generator.

Results and discussion

Figure 1a depicts the curve of resistance as a function of temperature in $Ge_{10}Sb_{90}$ and Er-doped $Ge_{10}Sb_{90}$. Initially, the resistance decreases slowly, which is attributed to the semiconductor-like behavior [21]. Then, the dramatically resistance drops are observed

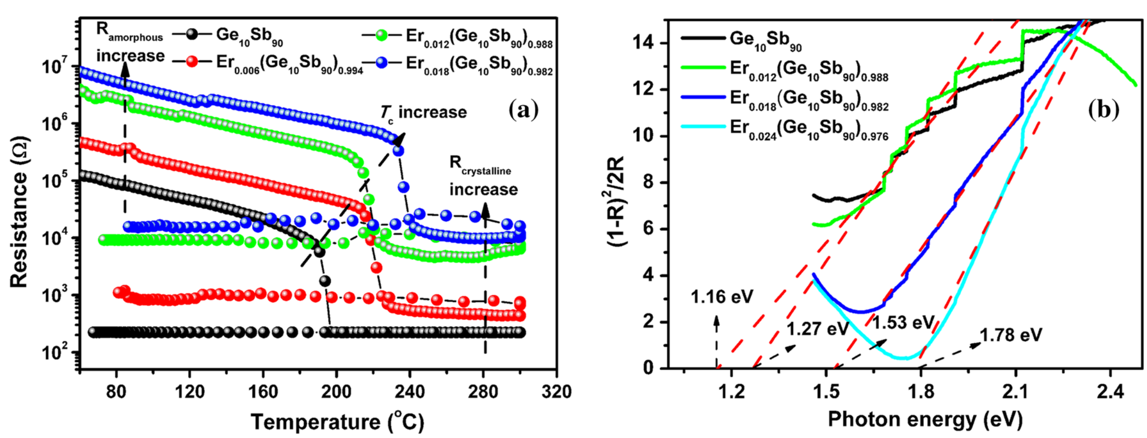

Figure 1 **a** The sheet resistance versus temperature curves for $Ge_{10}Sb_{90}$ and Er-doped $Ge_{10}Sb_{90}$ thin film with a heating rate of 20 °C/min. **b** The Kubelka–Munk function of the $Ge_{10}Sb_{90}$ and Er-doped $Ge_{10}Sb_{90}$.

until a certain value of crystallization temperature (T_c). It is apparently that with the increase in Er content, the T_c of $Er_x(Ge_{10}Sb_{90})_{1-x}$ increases. The crystallization process is inhibited by Er doping with T_c increasing from 189 °C of pure $Ge_{10}Sb_{90}$ film to 230 °C of $Er_{0.018}(Ge_{10}Sb_{90})_{0.982}$ film. It is usually considered that the high T_c will lead to better thermal stability. In order to confirm the crystallization state, the subsequent cooling process at the same rate was carried out. Figure 1a shows the resistances maintain in the low values, indicating the happening of amorphous-to-crystalline phase change. Gu et al. [22] have studied Ge_xSb_{100-x} films with various Ge contents, indicating T_c would increase with increasing the content of Ge. Raoux et al. [23] also have studied the Al-doped $Ge_{14}Sb_{86}$ thin films. Compared with these results, our work has the significant advantage of much few Er dopants.

In addition, Fig. 1a also shows that the resistances of amorphous ($R_{amorphous}$) and crystalline ($R_{crystalline}$) state of Er-doped $Ge_{10}Sb_{90}$ increase with increasing the Er content, indicating the decrease in writing current of PCM based on the Er-doped thin film [24]. Thus, it is considered that the Er dopants can significantly improve the stability and reduce the power consumption of the PCM device based on the Er-doped $Ge_{10}Sb_{90}$ film.

The diffuse reflectivity spectra of the amorphous $Er_x(Ge_{10}Sb_{90})_{1-x}$ films were measured at room temperature in the wavelength ranging from 400 to 2500 nm. The values of optical band gap energy (E_g) were determined from the intercept on the energy axis with zero absorbance as shown in Fig. 1b. The conversion of the reflectivity to absorbance data can be obtained by the Kubelka–Munk function (K–M) [25].

$$K/S = (1 - R)^2/2R \quad (1)$$

where R is the reflectivity, K is the absorption coefficient and S is the scattering coefficient. As shown in Fig. 1b, the E_g of pure $Ge_{10}Sb_{90}$ thin film is 1.16 eV. With the Er dopants, the E_g increases from the 1.27 eV of $Er_{0.012}(Ge_{10}Sb_{90})_{0.988}$ to 1.78 eV of $Er_{0.024}(Ge_{10}Sb_{90})_{0.976}$. Generally, the carrier density inside the semiconductors was proportional to $\exp(-E_g/2kT)$ [26]. Thus, an increase in the band gap would lead to the reduction in carriers, which made a major contribution to the increasing film resistivity after more Er doping, which was supported by the change trends of resistance curves in Fig. 1a.

In order to further evaluate the data retention of phase-change materials, the isothermal crystallization was employed in time-dependent resistance at different temperatures. Figure 2a shows the dependence of normalized resistivity on time for $Er_{0.018}(Ge_{10}Sb_{90})_{0.982}$ thin film isothermally measured at fixed temperatures. The other $Er_x(Ge_{10}Sb_{90})_{1-x}$ films are measured with the same way. The failure time can be defined as the time when the resistance decreases to half. Then, the 10-year data retention can be inferred by Arrhenius equation [25].

$$t = \tau \exp(E_a/K_B T) \quad (2)$$

where t, τ, E_a, K_B and T are the failure time, the pre-exponential factor, activation energy, Boltzmann's constant and the absolute temperature, respectively. It can be seen that the E_a of Er-doped $Ge_{10}Sb_{90}$ films increases from 3.22 to 4.15 eV with increasing the Er

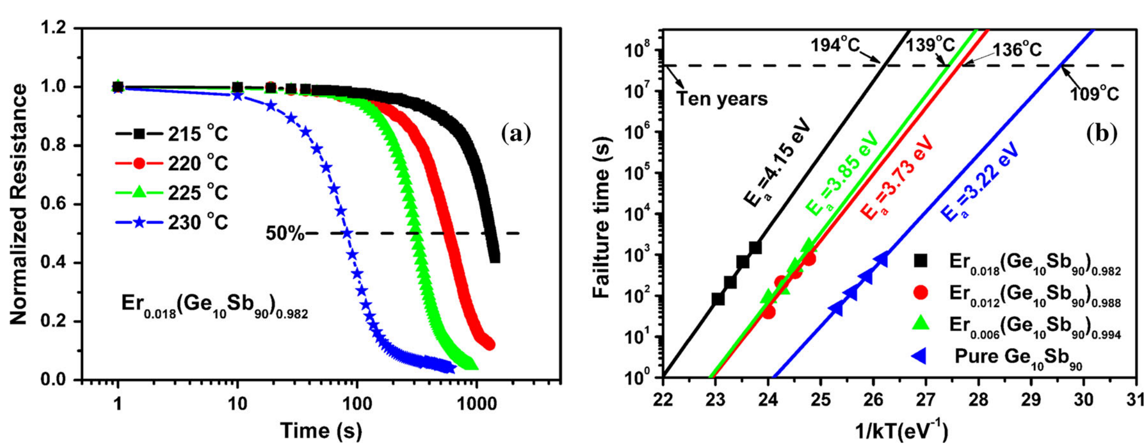

Figure 2 **a** Normalized resistance of $Er_{0.018}(Ge_{10}Sb_{90})_{0.982}$ thin film as a function of annealing time at various temperatures. **b** Plots of failure times as a function of reciprocal temperature of $Ge_{10}Sb_{90}$ and Er-doped $Ge_{10}Sb_{90}$ thin films.

Table 1 T_c, E_g, E_a and T_{ten} of pure $Ge_{10}Sn_{90}$ and Er-doped $Ge_{10}Sb_{90}$ thin films

	$Ge_{10}Sb_{90}$	$Er_{0.006}(Ge_{10}Sb_{90})_{0.994}$	$Er_{0.006}(Ge_{10}Sb_{90})_{0.994}$	$Er_{0.006}(Ge_{10}Sb_{90})_{0.994}$
T_c (°C)	190	214	214	232
E_g (eV)	1.16	1.27	1.53	1.78
E_a (eV)	3.22	3.73	3.85	4.15
T_{ten} (°C)	109	136	139	194

content. This results are also observed in Er-doped Sb film [20], Cu-doped Sb_4Te_2 [19] and Al-doped Sn_2Se_3 [27]. More importantly, the 10-year temperature (T_{ten}) increases with Er doping from the 109 to 194 °C with increasing the Er content. To compete with NOR flash memory, the data retention of 10 years for PCRAM at temperature should be higher than 125 °C [28]. From this perspective, PCM using Er-doped $Ge_{10}Sb_{90}$ films, which have 10-year retention at 136–194 °C, can well satisfy the requirement of consumer appliances and automotive systems.

Through the above analyses, it can be shown that the values of T_c, E_g, E_a and T_{ten} increased with increasing the Er content in Table 1. Rao et al. demonstrated that the improvement in thermal stability by doping is due to the doping element bonding to other elements [29]. We also have proved that the Er doping can significantly enhance the T_c, E_a and T_{ten} because of the Er–Sb bond [20]. Thus, it is inferred that the increase in the Er content appears to increase the T_c, E_g, E_a and T_{ten} due to the Er bonding to the Sb and Ge.

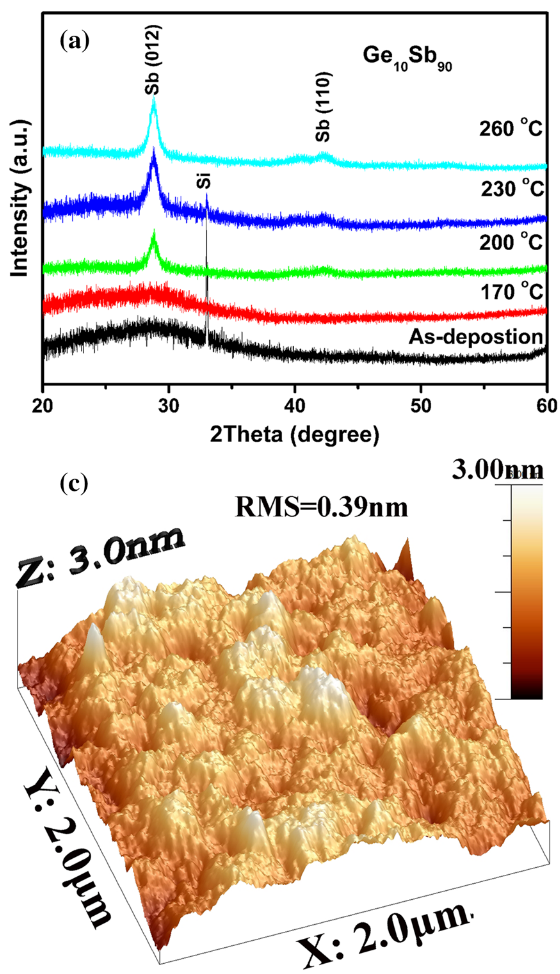

Figure 3 XRD patterns of the as-prepared and annealed **a** pure $Ge_{10}Sb_{90}$ and **b** Er-doped $Ge_{10}Sb_{90}$ thin films in Ar atmosphere for 5 min. AFM image of **c** $Ge_{10}Sb_{90}$ annealed at 300 °C and **d** $Er_{0.018}$ $(Ge_{10}Sb_{90})_{0.982}$ annealed at 300 °C.

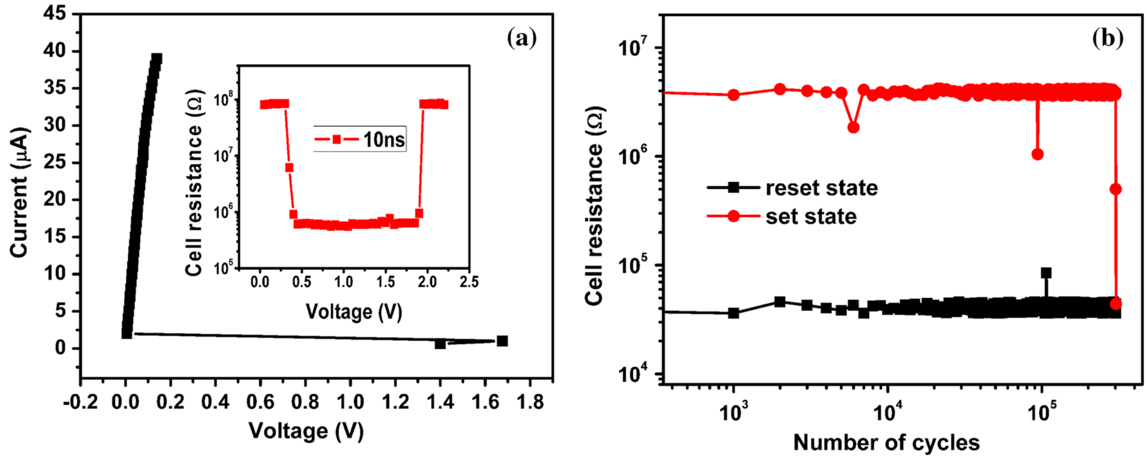

Figure 4 **a** Current–voltage characteristics of the PCM cell fabricated with the $Er_{0.018}$ $(Ge_{10}Sb_{90})_{0.982}$ thin films. *Inset* is the set and reset characteristic of PCM cell based on $Er_{0.018}$ $(Ge_{10}Sb_{90})_{0.982}$. **b** Endurance characteristic of PCM cell based on $Er_{0.018}$ $(Ge_{10}Sb_{90})_{0.982}$.

The crystalline structures and surface roughness were analyzed by XRD and AFM shown in Fig. 3. Obviously, these films have all crystallized into rhombohedral Sb (ICSD #409754) at the annealing temperature of 260 °C. More importantly, the amorphous structure of $Er_{0.01}(Ge_{10}Sb_{90})_{0.982}$ maintains until annealing temperature up to 200 °C, which is higher than the pure $Ge_{10}Sb_{90}$ of 170 °C. These results indicate that the Er dopants obviously inhabit the transition from amorphous to crystalline, meaning the improvement in thermal stability. Film surface roughness is vital for the device performance due to the electrode–film interface affected by the induced stress during the phase-change process [30, 31]. Figure 3c, d shows the AFM image of $Ge_{10}Sb_{90}$ and $Er_{0.018}(Ge_{10}Sb_{90})_{0.982}$ films annealing at 300 °C for 5 min. The root mean square (RMS) roughness calculated from the AFM images has slight change from 0.39 to 0.38 nm with Er doping. These values of RMS are lower that other phase-change film, such as Sb_2Te_3 [30] and $Sb_{70}Se_{30}$ [31], indicating well smooth surface for PCM devices.

The T-shaped PCM cells based on $Er_{0.018}(Ge_{10}Sb_{90})_{0.982}$ thin film were fabricated by using 0.18-μm complementary metal-oxide semiconductor (CMOS) technology. Figure 4a shows the current–voltage curves of PCM cell, and the inset of Fig. 4a reveals the resistance–voltage curves. As shown in Fig. 4a, the phase transition from the amorphous (reset state) into high conductive crystalline state (set state) can be easily observed. Figure 4a also shows when the current is up to 4 μA and the voltage is up to 1.7 V, the transition process occurred. The inset of Fig. 4a reveals that the set and reset voltage is 0.3 and 1.7 V with a 10-ns width pulse, indicating the phase-change speed faster than 10 ns. In general, when the pulse width is shorter, the voltage is larger than before. These results indicate that the PCM-based process lowers set and reset voltage than GST [32], and $Al_{1.3}Sb_3Te$ [33], meaning the lower power consumption than GST. In addition, it should be noticed that the Sb-rich films, such as GaSb [34] and GeSb [35], have very short crystallization time (<15 ns) due to their growth-dominated crystallization process instead of nucleation-dominated one. In this work, $Er_{0.018}(Ge_{10}Sb_{90})_{0.982}$ should have very fast phase-change speed (10 ns).

Figure 4b shows the endurance of the PCM cell based on $Er_{0.018}(Ge_{10}Sb_{90})_{0.982}$ thin films. It demonstrates a reversible switching up to 3.1×10^5 cycles without failure. Chen et al. [8] have studied the GeSb devices, revealing their cycling data showing 30000 set–reset cycles. Compared with this work, the device based on Er-doped $Ge_{10}Sb_{90}$ films processes excellent endurance, which is more decuple than the devices based on pure GeSb films.

Conclusion

In summary, the Er-doped $Ge_{10}Sb_{90}$ thin films have been fabricated and their phase-change behavior was investigated in this work. The T_c, E_a, $R_{amouphous}$ and $R_{crystalline}$ increase remarkable with Er doping, which lead to a better data retention and lower power consumption. The XRD tests reveal that the crystallization $Er_x(Ge_{10}Sb_{90})_{1-x}$ thin films shows only the existence of Sb phase. The AFM measurement shows the $Er_x(Ge_{10}Sb_{90})_{1-x}$ films process well surface roughness. More importantly, it has demonstrated that the ultrashort operation pulse (10 ns) can trigger set and reset operation switching in PCM cells based on $Er_{0.018}(Ge_{10}Sb_{90})_{0.982}$ film. The threshold voltage for the set and reset operation is only 0.3 and 1.7 V, respectively. Last but more importantly, more than 3.1×10^5 cycles of reversible switching has been achieved. All in all, the Er dopants improve the performance of $Ge_{10}Sb_{90}$ and the Er-doped $Ge_{10}Sb_{90}$ thin films are promising candidate for high-reliability and low-consumption PCM device applications.

Acknowledgements

The work was supported by University Natural Science Foundation of Jiangsu Province (No. 15KJB430012), National Science Foundation of China (Grant No. 11547142), Natural Science Foundation of Jiangsu Province (No. BK2015020024) and Changzhou Sci&Tech Program (Nos. CJ20159049, CJ20160028) and sponsored by Qing Lan Project.

References

[1] Loke D, Lee TH, Wang WJ, Shi LP, Zhao R, Yeo YC, Chong TC, Elliott SR (2012) Breaking the speed limits of phase-change memory. Science 336:1566–1569

[2] Welnic W, Wuttig M (2008) Reversible switching in phase-change materials. Mater Today 11:20–27

[3] Raoux S, Ielmini D (2009) Phase change materials and their application to nonvolatile memories. Chem Rev 110:240–267

[4] Simpson RE, Fons P, Kolobov AV, Fukaya T, Krbal M, Yagi T, Tominaga J (2011) Interfacial phase-change memory. Nat Nanotechnol 6:501–505

[5] Zhou X, Wu L, Song Z, Cheng Y, Rao F, Ren K, Song S, Liu B, Feng S (2013) Nitrogen-doped Sb-rich Si–Sb–Te phase-change material for high-performance phase-change memory. Acta Mater 61:7324–7333

[6] Golovchak R, Choi YG, Kozyukhin S, Chigirinsky Y, Kovalskiy A, Xiong-Skiba P, Trimble J, Pafchek R, Jain H (2015) Oxygen incorporation into GST phase-change memory matrix. Appl Surf Sci 332:533–541

[7] Zou H, Zhu X, Hu Y, Sui Y, Zheng L, Wu W, Zhai L, Xue J, Song Z (2016) Superlattice-like $Ga_{40}Sb_{60}$/Sb films with ultra-high speed and low power for phase change memory application. J Mater Sci Mater Electron. doi:10.1007/s10854-016-5991-2

[8] Chen YC, Rettner CT, Raoux S, Burr GW (2006) Ultra-thin phase-change bridge memory device using GeSb. In: Electron devices meeting, 2006. IEDM '06. International, pp 1–4

[9] Li Z, Hu Y, Wen T, Zhai J, Lai T (2015) Femtosecond laser-induced crystallization of amorphous N-doped Ge_8Sb_{92} films and in situ characterization by coherent phonon spectroscopy. J Appl Phys 117:135703

[10] Xia Y, Liu B, Wang Q, Zhang Z, Song S, Song Z, Yao D, Xi W, Guo X, Feng S (2015) Study on the phase change material Cr-doped Sb_3Te_1 for application in phase change memory. J Non-Cryst Solids 422:46–50

[11] Hu Y, Zhai J, Zeng H, Song S, Song Z (2015) Improvement of reliability and power consumption for SnSb4 phase change film composited with Ga_3Sb_7 by superlattice-like method. J Appl Phys 117:175704

[12] Chong TC, Shi LP, Zhao R, Tan PK, Li JM, Lee HK, Miao XS, Du AY, Tung CH (2006) Phase change random access memory cell with superlattice-like structure. Appl Phys Lett 88:743–747

[13] Jang MH, Park SJ, Lim DH, Cho MH, Do KH, Ko DH, Sohn HC (2009) Phase change behavior in oxygen-incorporated $Ge_2Sb_2Te_5$ films. Appl Phys Lett 95:012102

[14] Lee TH, Loke D, Elliott SR (2015) Microscopic mechanism of doping-induced kinetically constrained crystallization in phase-change materials. Adv Mater 27:5477–5483

[15] Chang PC, Chang CC, Chang SC, Chin TS (2014) Crystallization behavior of Si-added amorphous $Ga_{19}Sb_{81}$ films for phase-change memory. J Non-Cryst Solids 383:106–111

[16] You Y, Hosaka S (2012) Crystal growth suppression by N-doping into chalcogenide for application to next-generation phase-change memory. Key Eng Mater 497:101–105

[17] Fu J, Shen X, Nie Q, Wang G, Wu L, Dai S, Xu T, Wang RP (2013) Crystallization characteristics of Mg-doped $Ge_2Sb_2Te_5$ films for phase change memory applications. Appl Surf Sci 264:269–272

[18] Zhou X, Wu L, Song Z, Rao F, Ren K, Peng C, Song S, Liu B, Xu L, Feng S (2013) Phase transition characteristics of Al–Sb phase change materials for phase change memory application. Appl Phys Lett 103:072114

[19] Lu YG, Song SN, Song ZT, Rao F, Wu LC, Zhu M, Liu B, Yao DN (2012) Investigation of $CuSb_4Te_2$ alloy for high-speed phase change random access memory applications. Appl Phys Lett 100:193114

[20] Zou H, Zhu X, Hu Y, Sui Y, Wu W, Xue J, Zheng L, Song Z (2016) Improvement of the thermal stability of Sb thin film through erbium doping. CrystEngComm 18:6365–6369

[21] Hu Y, Feng X, Li S, Lai T, Song S, Song Z, Zhai J (2013) Superlattice-like $Sb_{50}Se_{50}/Ga_{30}Sb_{70}$ thin films for high-speed and high density phase change memory application. Appl Phys Lett 103:152107

[22] Gu Y, Zhang T, Song Z, Liu Y, Liu B, Feng S (2010) Characterization of the properties for phase-change material GeSb. Appl Phys A 99:205–209

[23] Raoux S, Salinga M, Jordan-Sweet J, Kellock A (2007) Effect of Al and Cu doping on the crystallization properties of the phase change materials SbTe and GeSb. J Appl Phys 101:044909

[24] Hu Y, Li S, Lai T, Song S, Song Z, Zhai J (2013) Fast crystallization and low power of Al-doped Sn_2 Se_3 thin films for phase change memory applications. J Alloy Compd 581:515–518

[25] Zheng Y, Cheng Y, Zhu M, Ji X, Wang Q, Song S, Song Z, Liu W, Feng S (2016) A candidate Zr-doped Sb_2Te alloy for phase change memory application. Appl Phys Lett 108:052107

[26] Hu Y, Zhu X, Zou H, Zhang J, Yuan L, Xue J, Sui Y, Wu W, Song S, Song Z (2016) Improved thermal stability of N-doped Sb materials for high-speed phase change memory application. Appl Phys Lett 108:223103

[27] Hu Y, Zhu X, Zou H, Lu Y, Xue J, Sui Y, Wu W, Yuan L, Song S, Song Z (2015) $Al_x(Sn_2Se_3)_{1-x}$ phase change films for high-temperature data retention and fast transition speed application. J Mater Sci Mater Electron 26:7757–7762

[28] He Z, Wu P, Liu R, Zhai J, Lai T, Song S, Song Z (2016) Superlattice-like SnSb4/Ge thin films for ultra-high speed phase change memory applications. CrystEngComm 18:1230–1234

[29] Ren K, Rao F, Song ZT, Lu SL, Peng C, Zhu M, Wu LC, Liu B, Feng SL (2014) Phase change material $W_{0.04}(Sb_4Te)_{0.96}$ for application in high-speed phase change memory. J Alloy Compd 594:82–86

[30] Wei F, Wang L, Kong T, Shi L, Huang R, Zhang J, Cheng G (2013) Amorphous thermal stability of Al-doped Sb_2Te_3 films for phase-change memory application. Appl Phys Lett 103:181908

[31] Wu W, Hu Y, Zhu X, Sui Y, Xue J, Yuan L, Song S, Song Z (2015) Improvement of the thermal stability and power consumption of $Sb_{70}Se_{30}$ through nitrogen doping. J Mater Sci Mater Electron 26:9700–9706

[32] Cheng X, Bo L, Zhi-Tang S, Song-Lin F, Bomy C (2005) Characteristics of Sn-doped $Ge_2Sb_2Te_5$ films used for phase-change memory. Chin Phys Lett 22:2929

[33] Cheng P, Liangcai W, Feng R, Zhitang S, Xilin Z, Min Z, Bo L, Dongning Y, Songlin F, Pingxiong Y, Junhao C (2011) Nitrogen incorporated GeTe phase change thin film for high-temperature data retention and low-power application. Scripta Mater 65:327–330

[34] Putero M, Coulet M-V, Ouled-Khachroum T, Muller C, Baehtz C, Raoux S (2013) Phase transition in stoichiometric GaSb thin films: anomalous density change and phase segregation. Appl Phys Lett 103:231912

[35] Huang CC, Gholipour B, Knight K, Ou JY, Hewak DW (2012) Deposition and characterization of CVD-grown Ge–Sb thin film device for phase-change memory application. Adv OptoElectron 2012:1–7